Selective Laser Sintering of Polyamide 12/Potassium Titanium Whisker Composites

Jinsong Yang,[1] Yusheng Shi,[1] Chunze Yan[2]

[1]*State Key Laboratory of Material Forming Simulation and Die and Mold Technology, Huazhong University of Science and Technology, Wuhan 430074, Hubei, China*
[2]*College of Materials Science and Chemical Engineering, China University of Geosciences. Wuhan 430074, Hubei, China*

Received 5 April 2007; accepted 16 November 2009
DOI 10.1002/app.31965
Published online 13 April 2010 in Wiley InterScience (www.interscience.wiley.com).

ABSTRACT: The excellent performance of potassium titanium whiskers (PTWs) reinforced plastics has been recognized; however, because of their large length-to-diameter ratio, they have not been applied in selective laser sintering (SLS). This article reports a new method for preparing polyamide 12 (PA12)/PTWs composite (PPC) powders for applications in SLS that uses a dissolution–precipitation process. The characteristics of the powders were evaluated. The results indicated that when the PTWs content of the composites was low (<10 wt %), the shape of the powder became more regular, and the particle diameter distribution became narrower. The crystallinity of PPC was 13 wt % higher than that of PA12. The sintering characteristics and mechanical properties of PA12 powder, glass-filled PA12 (GF–PA), and PPCs were compared. The results showed that the sintering characteristics of PPCs (10 or 20 wt % PTWs) were as good as those of PA12. The mechanical properties were greatly improved by PTWs. The maximum tensile strength, bending strength, and bending modulus of the composites containing 20 wt % PTW were 68.3 MPa, 110.9 MPa, and 2.83 GPa, respectively, and were much higher than those of PA12 and GF–PA. © 2010 Wiley Periodicals, Inc. J Appl Polym Sci 117: 2196–2204, 2010

Key words: fillers; polyamides; reinforcement; sintering

INTRODUCTION

Rapid prototyping (RP)[1,2] and whisker-reinforced composites[3,4] are of growing importance in manufacturing and materials, respectively. Whiskers are generally recognized as being free of internal defects such as dislocations because of their small diameter; furthermore, they possess improved properties while still being processable.[3–5]

RP techniques have been developed very quickly since their introduction. Traditionally, these techniques have been focused on areas in which the primary interest is generating a physical model of a component or system for the purpose of visualization. More recently, RP has evolved to applications in the manufacture of functional components for which a prototype is required to have sufficient mechanical integrity and surface quality for the purposes of handling and demonstration.[6–8] The mechanical properties become critically important, and they must be comparable to those obtained through the use of traditional manufacturing techniques to make the RP-based processes competitive.

The selective laser sintering (SLS) technique is one of the most widely used processes in RP. The SLS process is shown in Figure 1.[9,10] This process is based on the layer-by-layer principle. After an SLS system distributes a polymer powder in a layer over the part bed, the sintering process uses a laser to melt the powder, and the fluid flows together to create the object. In the unsintered areas, the powder remains loose and serves as a natural support for the next layer and the entire object under fabrication; hence, no additional support structure is required. Often, before the powder is sintered, the entire powder bed is heated to minimize thermal distortion and facilitate adhesion to the previous layer. As the process is repeated, layers of powder are deposited and sintered until the object is complete.

Polyamide-based composites have been proven to have great potential for the RP industry in fabricating functional parts;[10–13] however, the strength of classic sintered polyamide 12 (PA12) is only approximately 80% of that of an injection-molded polyamide

Correspondence to: Y. Shi (shiyusheng@263.net).
Contract grant sponsor: Natural Science Foundation of Hubei Province; contract grant number: 2005ABA181.
Contract grant sponsor: Special Fund for Basic Scientific Research of Central Colleges, China University of Geosciences (Wuhan, China); contract grant number: CUGL090305.

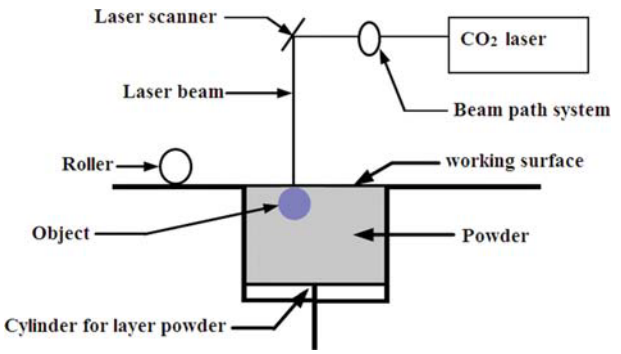

Figure 1 Schematic illustration of the SLS process. [Color figure can be viewed in the online issue, which is available at www.interscience.wiley.com.]

specimen. This SLS process limits the particle diameter to approximately 100 μm or less. The polymer particles in commercial glass-filled PA12 (GF–PA) have an average diameter of 48 μm; this makes fiber reinforcement difficult. The commercial composite contains glass at a 50 wt % concentration; this improves Young's modulus and the heat distortion temperature. However, these fillers reduce the strength and strain to failure.[14–16]

For these reasons, significant research efforts have been directed toward finding SLS materials with improved mechanical properties.[10,16–19] For example, Kim and Creasy[10] studied the clay-reinforced nanocomposite, and Wang et al.[19] studied the PA12/rectorite composite. However, it is difficult to disperse the nanofillers. Furthermore, increasing the amount of the nanofillers increases the viscosity of the polymer and affects the sintering characteristics.

Potassium titanium whiskers (PTWs; $K_2O{\cdot}6TiO_2$) are used as reinforcing materials because of their excellent chemical stability and mechanical properties.[4,5] In particular, their mechanical properties are considerably superior to those of traditional reinforcing materials such as glass and carbon fibers. They have small dimensions with average diameters and lengths of 1–2 and 10–40 μm, respectively, and they have been successfully applied to polypropylene, polyamide, poly(vinyl chloride), polycarbonate, polytetrafluoroethylene, and rubber.

However, PTWs are whiskers that possess a low apparent density of approximately 0.2–0.4 g/cm^3, and they tend to form aggregates; therefore, it is very difficult to distribute them uniformly into polyamide powders by mechanical mixing.[20] Furthermore, their structure would have a negative effect on the sintering characteristics.[16]

Therefore, we studied methods for preparing PTWs-reinforced PA12 materials for applications in SLS, and we researched the effect of PTWs on the sintering characteristics. Accordingly, we report here a new method for producing PA12/PTWs composite (PPC) powders in which PTWs are coated by PA12 in a dissolution–precipitation process.[20,21]

EXPERIMENTAL

Materials

PA12 (L1670 grade) was obtained from Degussa Co. (Germany); PTWs (Fig. 2) were obtained from Shanghai Whiskers and Composites Co., Ltd. (Shanghai, China). Before their use, they were treated with a silane coupling agent (WD-50, Wuhan University Silane New Material Co., Ltd., Wuhan, China). Glass beads were obtained from Xinhua Glass Beads Co., Ltd. (Yongxin, China); they had a diameter of 50–75 μm. The solvent was ethanol (containing 0.5% water and 1% butanone), which was obtained from Tianjin Damao Chemical Reagent Factory (Tianjin, China).

Preparation of the powders

The dissolution–precipitation procedure for the PA12 powder or PPC powder by which the PTWs were coated by PA12 was as follows. PA12 (or PA12 and PTWs), a solvent (1:7 wt/wt), and additives were added to a 10-L high-pressure reactor. The oxygen was pumped out; the mixture was stirred when the temperature reached 150°C for 1–2 h. Then, it was cooled at the rate of 10°C/h to 105°C until PA12 began to precipitate. The temperature was maintained at 105°C until the precipitation was complete (within 20 min); stirring was stopped, and the solvent was distilled.

The mechanical mixtures of the GF–PA powder and PTWs-filled PA12 (PTWs–PA) powder were obtained by the addition of PA12 and glass beads (or PA12 and PTWs) to a three-dimensional dynamic mixer with mixing for 4 h.

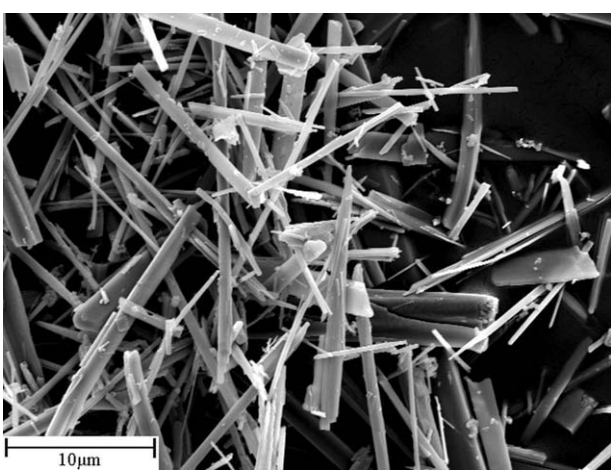

Figure 2 SEM micrograph of PTWs.

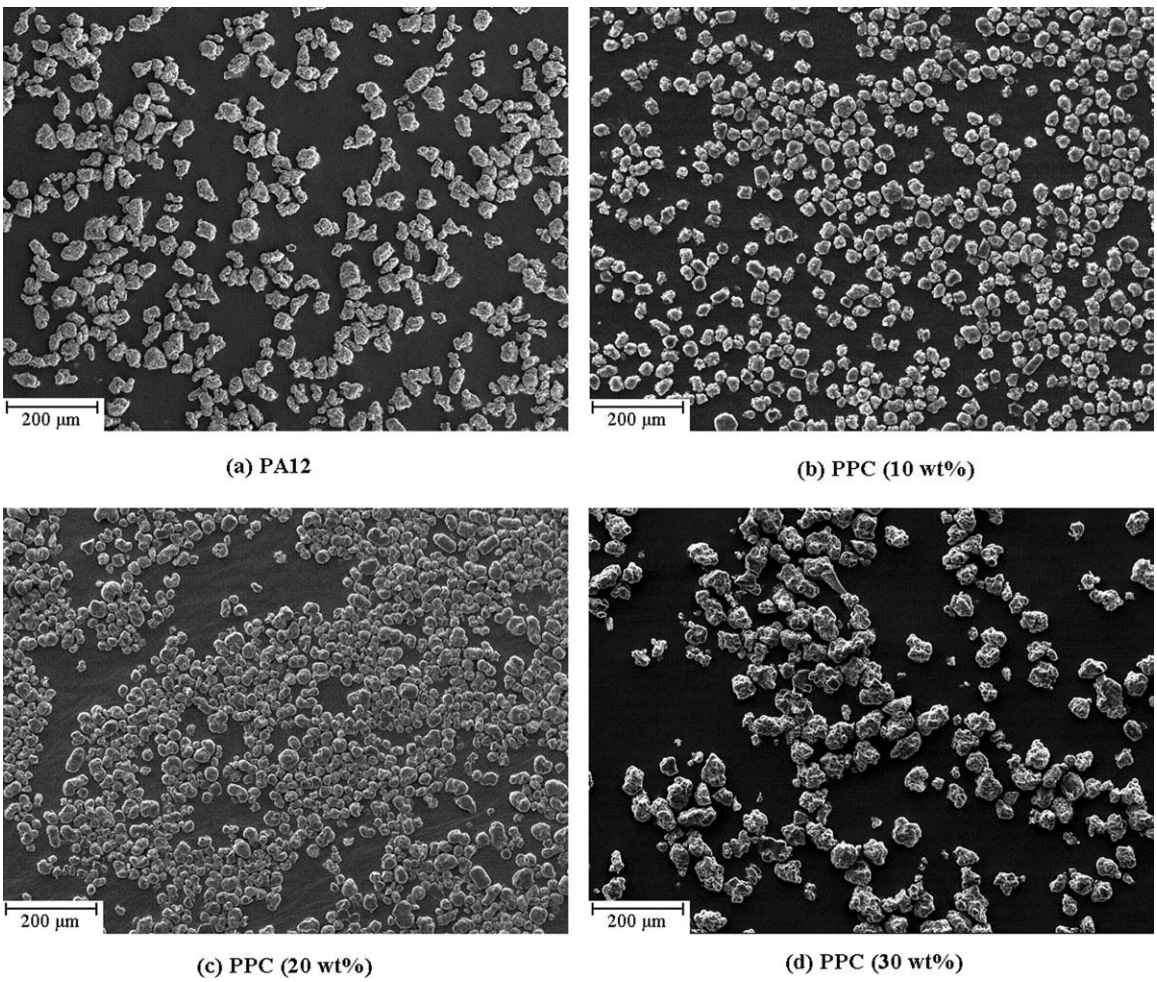

Figure 3 SEM micrographs of PA12 powders and PPC powders produced by dissolution–precipitation: (a) PA12, (b) PPC (10 wt %), (c) PPC (20 wt %), and (d) PPC (30 wt %).

Laser sintering experiments

The sintering experiments were performed in an HRPS-III SLS machine equipped with a 50-W CO_2 laser (48-5, Synrad, Inc., USA) constructed by the Huazhong University of Science and Technology (Wuhan, China); the powders were dried in a vacuum oven at 80°C for 8 h before use. The sintering parameters were as follows: laser power, 15–20 W; scanning speed, 2000 mm/s; scanning spacing, 0.1 mm; layer thickness, 0.1 mm; and part-bed temperature, 165–170°C.

Measurements

Mechanical properties

The tensile strength and bending strength were determined with a WDW-250 electronic test machine manufactured by Shenzhen Kaiqiangli Mechanical, Ltd. (Shenzhen, People's Republic of China), according to the ISO527/2-1993(E) and ISO178-1993(E) standards, respectively. The sizes of the specimens were 180 × 10 × 4 mm^3 and 55 × 6 × 4 mm^3, respectively. The tests were performed at room temperature with a crosshead speed of 5 mm/min. The impact strength was determined with an XJ-5 impact test machine (Chengde Mechanical, Ltd., Chengde, People's Republic of China) according to the ISO180-1993(E) standard. The size of the specimens was 63.5 × 10 × 12.7 mm^3. The average tensile strength, bending strength, and impact strength were obtained from six tests.

Morphological analysis

The morphologies of the raw powders and the sintered specimens were examined with an FEI Electron Optics (Holland) Sirion 200 scanning electron microscope at operating voltages below 20 kV. Such low voltages were chosen to minimize heat damage to the samples. All samples were sputter-coated with gold–palladium to avoid charging. To ensure that the PTWs were coated with PA12, an energy-dispersive X-ray spectroscopy (EDX) analysis system was used. The distribution of powder particles was obtained

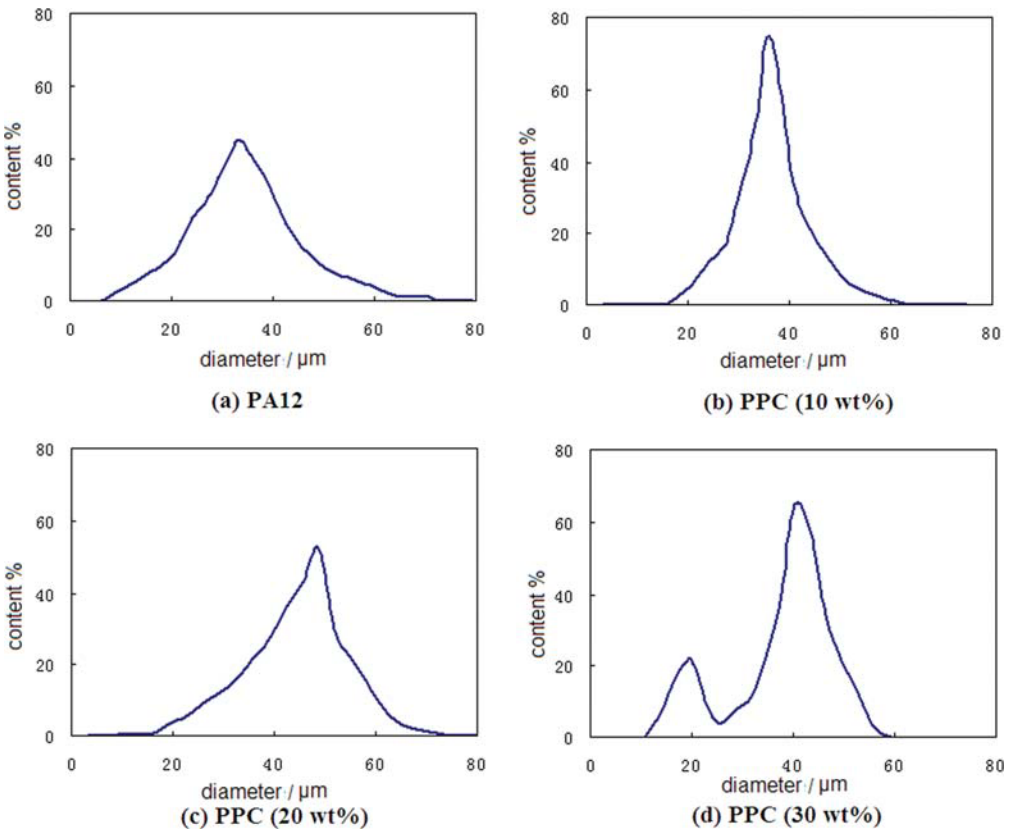

Figure 4 Particle diameter distribution curves of PA12 and PPC powders produced by dissolution–precipitation: (a) PA12, (b) PPC (10 wt %), (c) PPC (20 wt %), and (d) PPC (30 wt %). [Color figure can be viewed in the online issue, which is available at www.interscience.wiley.com.]

with a Vicom (USA) VDP-1750 image analysis system.

Thermal analysis

The melting and cooling behavior of both PA12 and PPC were studied with a PerkinElmer (USA) DSC-7. The heating rate was 10°C/min from room temperature to 200°C; then, cooling was performed at the same rate under the protection of nitrogen. The decomposition behavior was studied with a Netzsch (Erich NETZSCH GmbH & Co., Germany) Seiko thermogravimeter. The heating rate was 10°C/min from room temperature to 600°C under the protection of argon.

RESULTS AND DISCUSSION

Characteristics of the powders

A proper particle diameter and distribution are necessary for SLS. In previous studies,[16] a particle diameter of 20–50 μm was found to be ideal. If it is smaller than 20 μm, spreading the powder becomes difficult; if it is larger than 50 μm, the precision of the SLS parts and sintering characteristics deteriorate. Figures 3 and 4 show images and distributions of the PA12 and PPC powders produced by dissolution–precipitation.

According to Figures 3(a) and 4(a), the average diameter of the PA12 powders was 34.9 μm, and the distribution was wide; 7.3% of the particles were smaller than 20 μm, and 8.6% were larger than 50 μm.

The PPC (10 wt %) powders exhibited a narrow particle diameter distribution, as shown in Figures 3(b) and 4(b), with an average particle diameter of 36.7 μm. It can be explained that PTWs acted as heterogeneous nuclei[22,23] and changed the precipitation process of PA12 during the cooling period; this tended to produce powders of uniform diameters.

The PPC (30 wt %) powders are shown in Figures 3(d) and 4(d). The particle diameter distribution was not uniform; it exhibited two peaks. The main peak was at 40.69 μm, and the other was at 19.80 μm. The surfaces of the particles were very rough, and there were many pores in the particles. This appears to be the result of the random conglomeration of many small particles.

This can be explained as follows. The PTWs tended to aggregate, and it was difficult to disperse them well in the solvent as its concentration increased.[20] The PTWs spread directionally, and there were several growing points for one particle. PA12 precipitated around these growing points; as a result, a large particle resembled a random conglomeration of

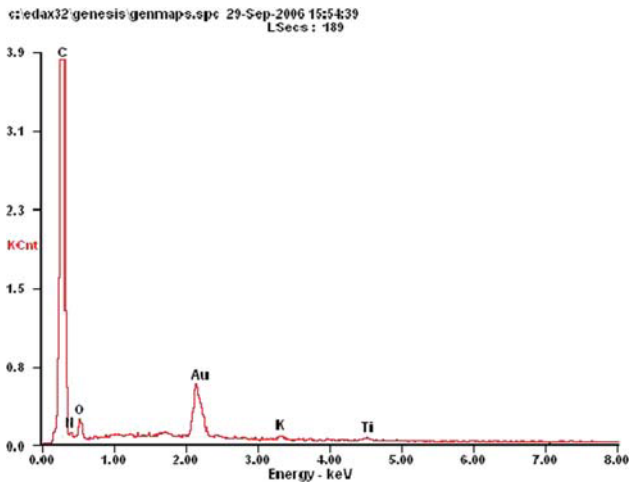

Figure 5 EDX patterns of PPC powders with 20% PTWs. [Color figure can be viewed in the online issue, which is available at www.interscience.wiley.com.]

several small particles. When the solvent trapped by PA12 was eliminated, the pores appeared. The small peak at 19.80 μm in the particle diameter distribution for PPC (30 wt %) was the contribution of dispersed PTWs (which had not aggregated) or PTWs possessing a smaller number of growing points.

There were no free PTWs in the powders shown in Figure 3(b–d); this indicates that all the PTWs were coated by PA12 in PPC powders. This result was also confirmed by the EDX analysis for one powder particle, as shown in Figure 5. According to Figure 5, the energy peak at 3.3 keV was the characteristic peak for potassium, and the peak at 4.5 keV was characteristic for titanium; the contents were 3.41 and 4.47 wt % for potassium and titanium, respectively. The existence of potassium and titanium indicated that there were PTWs in the powder particles; that is, PTWs were coated by PA12.

Thermal transition temperatures

Table I summarizes the detailed results obtained from the differential scanning calorimetry (DSC) experiments shown in Figure 6. Figure 6 shows the heating and cooling curves of PA12 and PPC (10, 20, and 30 wt %) powders from the DSC experiments. From the melting curves, we can observe that there was only one peak melting temperature for the three materials. This indicates that there was only one crystalline phase.

From Table I, the crystallinity index (CI) could be determined.[24] For a composite, *crystallinity* refers only to the polymer crystallinity; then, the amounts of fillers should be removed. CI was determined as follows:

$$\mathrm{CI} = (\Delta H_m/\Delta H_m^0) \times 100/(1-f) \quad (1)$$

where ΔH_m is the heat of fusion of the sample, ΔH_m^0 is the heat of fusion of purely crystalline PA12 (which is an invariable value), and f is the filler weight percentage. The CI values of PPCs containing 10, 20, or 30 wt % PTW were about 13% higher than those of the PA12 powers. This indicates that heterogeneous nuclei would promote crystallization.[22]

By comparing the cooling curves, we obtained the overall time of crystallization (t_c).[25] The calculated t_c values are 0.82, 0.72, 0.72, and 0.71 min for PA12, PPC (10 wt %), PPC (20 wt %), and PPC (30 wt %), respectively; this indicates that the crystallization speed of PPC was only about 0.1 min faster than that of PA12, and the initial crystallization temperature (T_{ic}) was similar. Hence, the crystallization speed would not significantly affect the laser sintering characteristics of PPC powders.

Laser sintering characteristics

There are two periods in the laser sintering of materials:[26–29] the melting period and the solidifying period. In the melting period, powder particles absorb the laser power and melt, and air in the particles is expelled; accordingly, the density increases from approximately 0.4 g/cm^3 (the powder apparent density) to approximately 1 g/cm^3. Although it exhibits a large shrinkage value, the shrinkage mostly occurs along the height direction without distortion, as the fusion can flow freely. During the solidifying period, distortion occurs as shrinkage stress if the part-bed temperature cannot be controlled well because the sintering parts cannot flow in this period. There are two forms of shrinkage: thermal shrinkage and crystallization shrinkage. Crystallization shrinkage occurs to a greater extent (the melt shrinkage ratio is

TABLE I
Thermal Transition Temperatures of the PA12 and PPC Powders

	T_{im} (°C)	T_m (°C)	T_{em} (°C)	ΔT_m (°C)	T_{ic} (°C)	T_{ec} (°C)	ΔH_m (J/g)	ΔH_c (J/g)
PA12	176.5	181.8	184.1	7.6	152.9	144.7	81.9	−51.9
PPC (10 wt %)	178.0	182.6	184.5	6.5	152.5	145.3	83.3	−50.0
PPC (20 wt %)	176.7	181.7	183.2	6.5	153.2	146.0	74.1	−43.7
PPC (30 wt %)	176.7	181.6	183.1	6.4	153.2	146.1	64.7	−37.8

T_m = melting temperature; T_{em} = the end of melting temperature; T_{ec} = the end of crystallization temperature; ΔH_c = crystallization enthalpy.

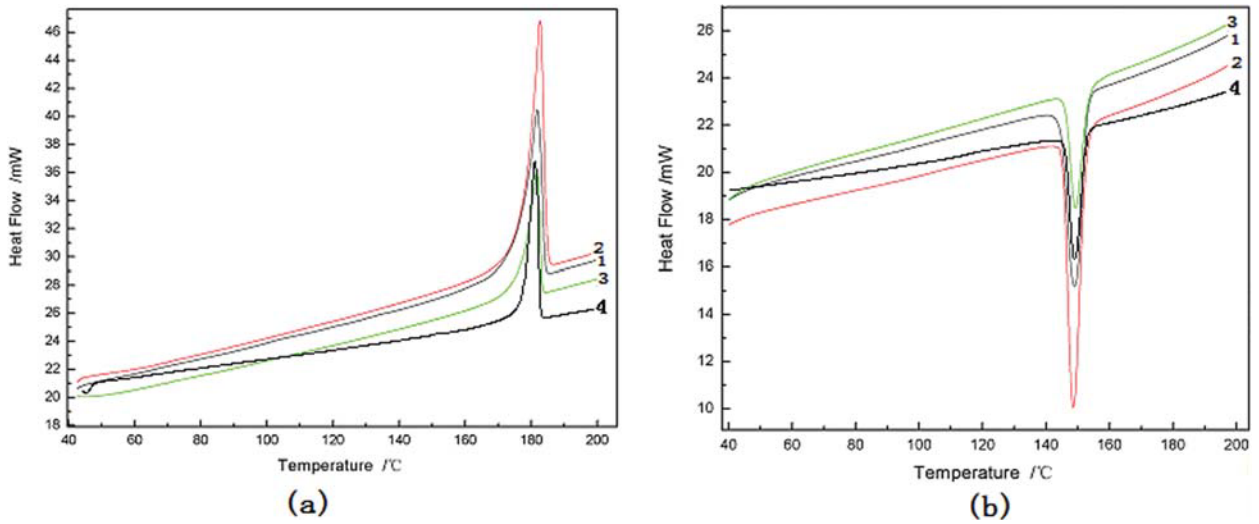

Figure 6 DSC results for PA12 and PPC powder with different PTWs contents: (a) melting temperatures found during heating from room temperature and (b) crystallization temperatures found during cooling from the melt for (1) PA12, (2) PPC (10 wt %), (3) PPC (20 wt %), and (4) PPC (30 wt %). [Color figure can be viewed in the online issue, which is available at www.interscience.wiley.com.]

approximately 1–2% for PA12),[30] and it occurs in a shorter temperature range. It is the main source of the shrinkage stress that induces distortion.

Before a powder is sintered, the entire powder bed is heated to prevent the sintering part from distorting by minimization of the temperature difference between the sintered parts and the surrounding environment. A higher temperature of the entire powder bed, which is known as the part-bed temperature, will decrease the crystallization speed; hence, the shrinkage stress can be released freely, and distortion is prevented.

There is a range of part-bed temperatures (the sintering temperature window) at which a powder can be sintered without distortion and the polymer powder will not coalesce spontaneously. Theoretically, the sintering temperature window is the range of temperatures within which the polymer powder begins to melt and the melt begins to crystallize. The theoretical sintering temperature window (ΔT_0) can be calculated with the following equation:[28]

$$\Delta T_0 = T_{im} - T_{ic} \quad (2)$$

where T_{im} is the initial melting temperature. T_{im} and T_{ic} were obtained from the DSC curves of the polymer powders (Fig. 6), and they are listed in Table I.

In fact, the coalescence temperature is lower than theoretical temperature T_{im}. Because semicrystalline polymers such as PA12 contain crystalline regions and amorphous regions, the amorphous regions appear to be viscous below the melting point.

Moreover, the minimum sintering temperature is restricted by many other factors, such as the powder shape, particle diameter, crystallization speed, and thermal transition of the polymer. Therefore, the available sintering temperature is much narrower than that calculated theoretically. It can be obtained by the measurement of the lowest agglomeration temperature and the highest distortion temperature of the powder. The previous reports[18,28] and this research show that the available sintering temperature window (ΔT_1) is only 1–2°C. The available sintering temperature of PA12 is 168–169°C. Among all the fillers, glass can extend the sintering temperature window. Its available sintering temperature is 167–170°C.[16] This is one of the most important reasons that GF–PA is the only polyamide composite that is now commercially applied. The ΔT_1 values are listed in Table II.

For all fillers, globular fillers such as glass are favorable for sintering, but fibrous fillers such as PTWs are not favorable. Because of the large length-to-diameter ratio, PTWs significantly affect the sintering characteristics. PPC powders with 10–20 wt % PTWs had sintering characteristics as good as those of PA12 powders. The sintering layer had a regular boundary and a smooth surface without distortion. When the PTWs content reached 30 wt %, the

TABLE II
Theoretical and Available Sintering Temperatures of PA12 and the PA12-Based Composites

	PA12	GF–PA (40 wt %)	PPC (20 wt %)
ΔT_0 (°C)	23.6	23.6	23.5
ΔT_1 (°C)	1–2	3–4	1–2
Range of ΔT_0 (°C)	152.9–176.5	152.9–176.5	153.2–176.7
Range of ΔT_1 (°C)	168–169	167–170	168–169

Figure 7 SLS specimen of PPC with 30% PTWs. [Color figure can be viewed in the online issue, which is available at www.interscience.wiley.com.]

sintering layer surface was smooth, but the boundary was zigzagged. This did not affect the SLS process, but the side of the sample was not sufficiently smooth (Fig. 7). However, for PTWs–PA powders with 20 wt % PTWs, the sintered region was distorted by the presence of many pores. This affected the sintering process so seriously that the process could not be continued.

Therefore, the conclusion can be drawn that the shape of the particles greatly affected the sintering characteristics. This phenomenon can be explained as follows. The PTWs had a low apparent density of approximately 0.2–0.4 g/cm^3 and tended to aggregate, so it was very difficult to achieve a uniform distribution in PA12 powders by mechanical mixing. Furthermore, it was very difficult for aggregated PTWs to be wetted by the PA12 melt, and the melt would have been distorted because of surface tension.[31]

However, when the fillers were coated well by PA12 (e.g., PPC powders), the sintering characteristics were determined only by the composite powder particles, whose shape was determined by the PTWs content: when the PTWs content was low (<10%), the shape of the particles was regular, and good sintering characteristics were obtained. However, with an increase in the PTWs content, the particle shape became irregular, and the sintering characteristics deteriorated.

Mechanical properties

The mechanical properties of the samples are listed in Table III. For GF–PA (40 wt %), the tensile strength remained constant, whereas the bending strength increased by 19.5% and the bending modulus increased by 61.4% with respect to PA12. However, this result was unsatisfactory because the impact strength significantly decreased. The impact strength of GF–PA (40 wt % glass) was only 50.3% of that of PA12.

For PPC samples, the mechanical properties improved significantly with PTWs. For the PPC (20 wt %) samples, the maximum tensile strength, bending strength, and bending modulus increased by 55, 118, and 158% with respect to PA12, respectively. The impact strength was 89.3% of that of the PA12 samples but 169% of that of the GF–PA (40 wt %) samples.

Therefore, we can conclude that PTWs are much better than glass beads as reinforcing fillers for PA12 in the SLS process.[20]

Morphology of the impact fracture surface

Scanning electron microscopy (SEM) images of impact-fractured PA12 and GF–PA samples are shown in Figure 8. The surface was coarse for PA12 samples and smooth for GF–PA samples, except that there were many pullout glass beads and pores. This indicates that the glass bead was not firmly fixed with PA12. Consequently, the mechanical properties of the GF–PA samples were unsatisfactory.

The impact fracture of PPC samples is shown in Figure 9. The surface was not regular as there were some cracks and pores. Although there were pullout whiskers, as shown in Figure 9(b), the whiskers surface was coarse, and most of the whiskers were coated by PA12. This indicates that PTWs exhibited better bonding to PA12.

As shown in Table III, the optimum amount of PTWs was only 20%. This can be explained from Figure 9(c,d) as follows: the pullout whiskers aggregated, but, as is well known, the fillers had to be dispersed well to acquire the optimal properties.

Thermal properties

Figure 10 shows the thermogravimetry (TG) curves of the PA12 powders and the PPC (20 wt %) powders. The initial degradation temperature was 323°C for PA12 powders and 360°C for PPC (20 wt %). The mass loss was approximately 50% for PA12 and 31% for PPC (20 wt %) at 450°C. This indicates that PTWs improved the stability of PA12.

TABLE III
Mechanical Properties of the PA12, GF–PA, and PPC Samples

		GF–PA				PPC	
	PA12	30 wt %	40 wt %	50 wt %	10 wt %	20 wt %	30 wt %
Tensile strength (MPa)	44.0	44.5	45	45.3	52.5	68.3	52.7
Impact strength (kJ/m^2)	37.2	20.9	18.7	15.3	34.3	31.2	20.3
Blending strength (MPa)	50.8	59.8	60.7	59.4	72.2	110.9	85.3
Blending modulus (MPa)	1.14	1.68	1.84	1.81	1.52	2.83	2.68

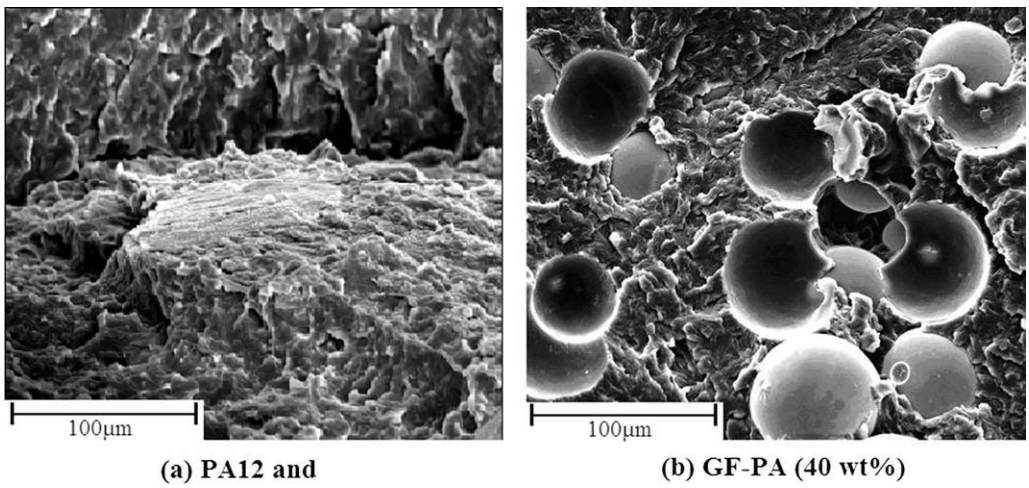

Figure 8 SEM micrographs showing the impact microstructures of (a) PA12 and (b) GF–PA (40 wt %).

CONCLUSIONS

A dissolution–precipitation process has been developed to produce PPC powders for applications in SLS. By this method, the whiskers are well coated by PA12; a large length-to-diameter ratio is maintained, while deterioration of sintering characteristics is avoided. This is a good method for producing composite powders for applications in SLS.

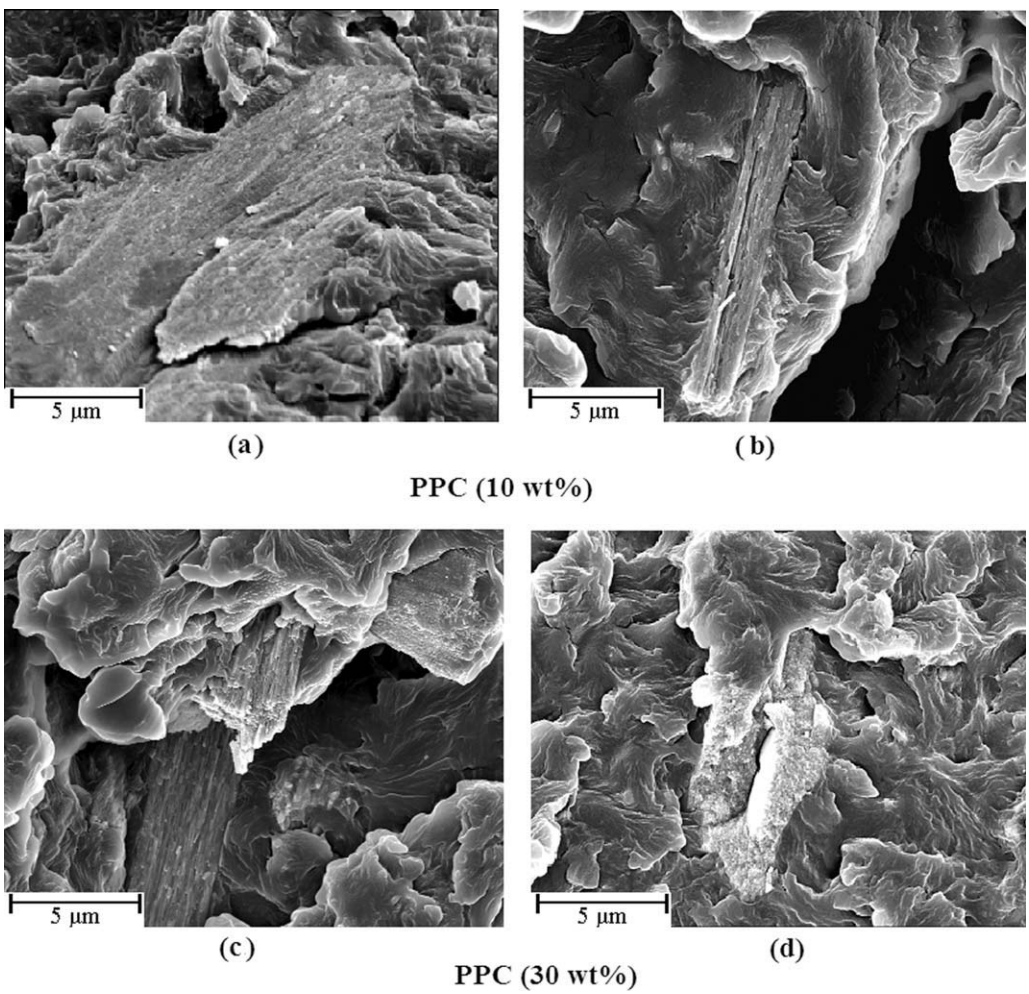

Figure 9 SEM micrographs showing the impact microstructure of PPC with different PTWs contents: (a,b) 10 and (c,d) 30 wt %.

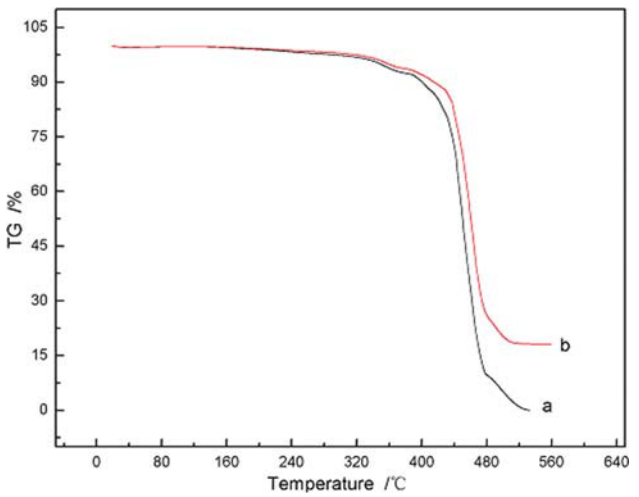

Figure 10 TG curves of (a) PA12 and (b) PPC (20 wt %). [Color figure can be viewed in the online issue, which is available at www.interscience.wiley.com.]

PTWs are much better than glass as filler materials for PA12 in SLS. They significantly improve the tensile strength, bending strength, and bending modulus of PA12 composites with little effect on the impact properties. The maximum tensile strength, bending strength, and bending modulus of a composite containing 20 wt % PTW were 68.3 MPa, 110.9 MPa, and 2.83 GPa, respectively.

Producing regular PA12 composite powders for SLS by a dissolution–precipitation process is favorable. Some other reinforced material can be used for SLS in this way.

References

1. Pham, D. T.; Gault, R. S. Int J Machine Tools Manuf 1998, 38, 1257.
2. Hopkinson, N.; Dickens, P. Rapid Prototyping J 2001, 7, 197.
3. Lu, J. Z.; Lu, X. H. J Appl Polym Sci 2001, 82, 368.
4. Tjong, S. C.; Meng, Y. Z. Polymer 1998, 39, 5461.
5. Qu, M. J.; Jian, X. G.; He, W. Compos Mater Sci Technol 2004, 112, 34.
6. Seitz, S.; Crommert, S.; Esser, K. J. SPIE Proc 1997, 3102, 106.
7. Holtzberg, W. M. U.S. Pat. 6,103,156 (2000).
8. Dickens, E. D., Jr. U.S. Pat. 5,648,450 (1997).
9. Kumar, S. JOM 2003, 55, 43.
10. Kim, J.; Creasy, T. S. Polym Test 2004, 23, 629.
11. Zarringhalam, H.; Hopkinson, N.; Kamperman, N. F. Mater Sci Eng A 2006, 435, 172.
12. Salmoria, G. V.; Leite, J. L.; Ahrens, C. H. Polym Test 2007, 26, 361.
13. Caulfield, B.; McHugh, P. E.; Lohfeld, S. J Mater Process Technol 2007, 182, 477.
14. Childs, T. H. C.; Tontowi, A. E. J Eng Manuf 2001, 215, 1481.
15. Chung, H.; Das, S. Mater Sci Eng A 2006, 437, 226.
16. Muo, J. H.; Shi, Y. S., Yang, J. S. Rapid Prototyping and Rapid Mold. Electronic Industry Press: Beijing, 2006.
17. Yuan, Q.; Jiang, W.; An, L.; Li, R. K. Y.; Jiang, Z. J Appl Polym Sci 2003, 89, 2102.
18. Mazzoli, A.; Moriconi, G.; Giuseppe, M. Mater Des 2007, 28, 993.
19. Wang, Y.; Shi, Y.; Huang, S. Proc Inst Mech Eng Part L 2005, 219, 11.
20. Chen, E.; Chen, D. Polym Mater Sci Eng 2006, 22, 20.
21. Cui, X. L. China Fine Chem 1996, 13, 41.
22. He, S. Q.; Li, Y.; Zhu, C. S. China Plast Ind 2004, 32, 39.
23. Li, Z.; Xiao-Xia, M.; Chen, S.-M. J Shenyang Polytech Univ 1999, 21, 367.
24. Khanna, Y. P.; Kuhn, W. P. J Polym Sci Part B: Polym Phys 1997, 35, 2219.
25. Wu, Z.; Zhou, C.; Zhu, N. Polym Test 2002, 21, 479.
26. Tontowi, A. E.; Childs, T. H. C. Rapid Prototyping J 2001, 7, 180.
27. Yang, H. J.; Wang, P. J.; Lee, S. H. Int J Machine Tools Manuf 2002, 42, 1203.
28. Martin, S. M. S. Ph.D. Thesis, University of Texas at Austin, 1991.
29. Gibson, I.; Shi, D. P. Rapid Prototyping J 1997, 3, 129.
30. Shi, Z. P. Manual of Polyamide Resin; Petro China: Beijing, 1994.
31. Nikolay, K.; Sergei, T.; Mozzharov, E. Rapid Prototyping J 2004, 10, 78.